ZERO BRINE

D4.4 Waste heat recovery opportunities in the precipitated silica industry

December 2020

FINAL

The ZERO BRINE project (www.zerobrine.eu) has received funding from the European Union's Horizon 2020 research and innovation programme under grant agreement No 730390.

Deliverable X.X	Title of deliverable
Related Work Package	WP4-Promoting circular economy in the chemical sector: an innovative scheme in the precipitated silica industry to recover water, sodium sulphate, waste heat acids and alkalis
Deliverable lead	Eurecat
Author(s)	Jordi Macià (Eurecat)
Contact	jordi.macia@eurecat.org
Reviewer	Henri Spanjers (Delft University of Technology)
Grant Agreement Number	730390
Funding body	Horizon 2020 Framework Programme
Start date	1.6.2017
Project Duration	48 months
Type of Delivery (R, DEM, DEC, Other)[1]	R = Report
Dissemination Level (PU, CO, CI)[2]	Pu = Public
Date Last update	23 December 2020
Approved by	Sandra Meca
Website	www.zerobrine.eu

Revision no	Date	Description	Author(s)
0.1	20.02.2018	First draft	Joan Farnós (CTM)
0.2	22.12.2020	Update according reviewer comments	Jordi Macià (Eurecat)
1.0	23.12.2020	Final version	Sandra Meca (Eurecat)

The ZERO BRINE project has received funding from the European Commission under the Horizon 2020 programme, Grant Agreement no. 730390. The opinions expressed in this document reflect only the author's view and do not reflect the European Commission's opinions. The European Commission is not responsible for any use that may be made of the information it contains.

[1] **R**=Document, report; **DEM**=Demonstrator, pilot, prototype; **DEC**=website, patent fillings, videos, etc.; **OTHER**=other

[2] **PU**=Public, **CO**=Confidential, only for members of the consortium (including the Commission Services), **CI**=Classified

Executive Summary

This document presents the results of Task 4.2. The task consists in proposing and assessing a waste heat recovery system (WHRS) for the recovery of waste heat available at the silica industry, Industrias Químicas del Ebro S.A. (IQE). Recovered energy will be used to supply cooling demand of the eutectic freeze crystallizer. This technology is one of the evaluated in the porject to recover the Glauber's salt ($Na_2SO_4 \cdot 10H_2O$) contained in the wastewater of the silica production process.

First of all, a review of the WHR technologies is carried out to identify the most suitable ones to supply Eutectic Freeze Crystallizer energy demand. The EFC consumes cooling energy at -5°C. The technologies spotted cover different options such as heat to power: Rankine Cycle, Organic Rankine Cycle (ORC), Kalina Cycle, or the Thermoelectric Refrigeration; heat pump technology electrically driven and thermally driven. Thermally driven cooling technologies include Absorption, Adsorption and Ejection Heat Pump technologies. Most of them are not suitable for the silica industry application because of temperature range or are still not available in the market. Single effect absorption chillers can provide sub-zero cooling temperatures with low grade input heat of 75°C.

As it comes to the part of up-scaling the whole WHR processes, it has been sized for a reference production of 20,000 tonnes/year of $Na_2SO_4 \cdot 10H_2O$. The main share of waste heat available in the silica industry comes from the silica gas dryers producing exhaust gas from 95 to 130°C at 55,500 kg/h mass flow rate, which stands for an average thermal power of 600 kW_{th}. The absorption technology (Absorption Chiller, AC) is selected as the state of the art. According to manufacturer Johnson & Controls Ltd, absorption chillers that can achieve the -5°C of chilled water with a 100°C heat source are available in the market. For that, some customizations have to be done to a commercial model that allow to use a mixture of glycol and LiBr-Water as a carrier fluid, in order to achieve sub-zero temperatures.

To calculate EFC performance in an integrated waste heat recovery system (WHRS), the EFC model developed by Eurecat in WP5 and presented in document D5.2, has been implemented in Matlab. The model has coefficients of crystal growth rate and nucleation rate of the crystals that need to be adjusted experimentally. This will be done in future tasks of the project by TU Delft and SEALEAU.

Results indicated that coupling AC unit with the waste heat available from the gas-dryers, a reduction of 72% on energy consumption could be achieved compared to a conventional VC electric cycle. The investment has a payback period of 5 years.

Contents

List of figures

List of tables

1. Overview of the ZERO BRINE project

The ZERO BRINE project aims to facilitate the implementation of the Circular Economy package and the SPIRE roadmap in various process industries by developing necessary concepts, technological solutions and business models to redesign the value and supply chains of minerals and water while dealing with present organic compounds in a way that allows their subsequent recovery.

Minerals and water will be recovered from saline impaired effluents (brines) generated by the process industry while eliminating wastewater discharges and minimizing the environmental impacts of industrial operations through brines (ZERO BRINE). ZERO BRINE brings together and integrates several existing and innovative technologies to recover products of high quality and sufficient purity to represent good market value.

WP4 aims at demonstrating circular economy in the chemical sector, specifically in a silica industry. To do this, an innovative process based in high pressure membrane filtration (NF/RO) using regenerated membranes and a crystallization stage will be applied to treat saline wastewater generated in this industry. Water and Na_2SO_4 will be recovered from the wastewater. In order to reduce energy consumption, waste heat recovery strategies will be also developed from a theoretical point of view.

2. Objectives

This study reflects the work done in Task 4.2 under WP4. The objectives of the task are:

- To assess the waste heat recovery from the silica industry to recover Glauber's salt from the wastewater of the silica production process. The salt recovery technology selected is the innovative EFC that permits to obtain pure salt with a lower energy cost than the conventional technology Evaporation-Crystallization.
- To identify and assess the more suitable waste heat recovery technologies that can supply the cooling demand of the EFC.

3. Introduction

One of the four demonstration sites of ZERO BRINE project is located at Industrias Químicas del Ebro S.A. (IQE) in Spain. IQE Group is an industrial chemical group composed by three companies: DESILSA, SIMAL and *Industrias Químicas del Ebro, S.A*. IQE, which has its headquarters in Zaragoza, began its business activity in 1958. It is specialized in basic inorganic chemistry and manufactures sodium and

potassium silicates, metasilicate, zeolites, sodium and potassium aluminates, aluminum sulphate, precipitated silica, aluminum silicate and amorphous aluminum hydroxide.

In the silica production process high amounts of water and reagents (NaOH, H_2SO_4, sand) are consumed and high amounts of waste streams with high salinity are produced. These streams contain high concentration of sodium sulphate and are normally discharged to natural watercourses (rivers, sea) after passing through wastewater treatment plants, with a high cost and environmental impact associated. In addition, high amounts of energy are required for spray-dryers in the manufacturing of SiO_2. As a result, waste heat streams are available, so its recovery can be considered.

ZERO BRINE aims to evaluate an innovative treatment process based on circular economy strategy. This treatment for saline wastewaters aims to recover water and sodium sulphate to further valorize them either in the production process at IQE or in other industries. The implementation of the new treatment process will allow achieving zero liquid discharge and promoting water reuse, while reducing costs derived from water consumption and wastewater management. Figure 1 shows the circular economy strategy developed in ZERO BRINE.

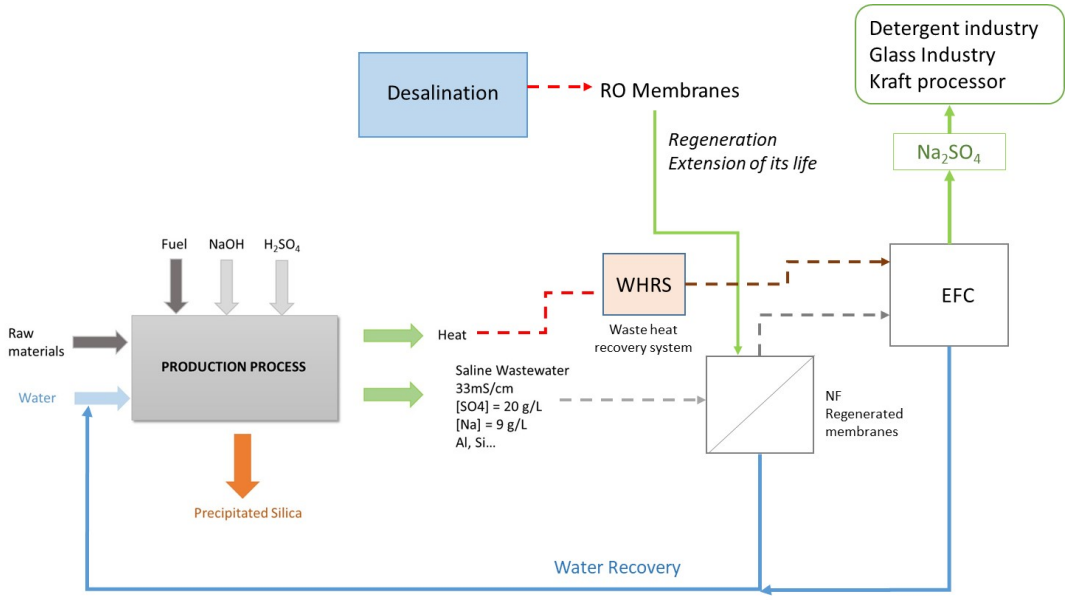

Figure 1: Proposed circular economy scheme for IQE by ZERO BRINE.

In ZERO BRINE solution, crystallization is the more energy-demanding stage in comparison with membrane stage. EFC presents several advantages in comparison with conventional crystallization systems based on evaporation systems: 1) lower energy requirements as latent heat of ice formation (334 kJ/kg) is 6 times lower than the evaporation one (2264 kJ/kg);.2) higher purity of recovered salts. Even all these advantages, waste heat recovery systems would allow to reduce energy consumption of this stage. A wide offer of technologies for waste heat recovery (WHR) exists either to transform it to

electrical power, to heating or cooling. In this document the research done to find the optimal combination of technologies that maximize both waste heat and sodium sulphate recovery for the specific case of the IQE plant is presented.

4. State of the Art of waste heat recovery technologies

Energy demand for EFC technology is to provide cooling at -5°C as it will be described in further sections. Energy recovery technologies, which can produce cooling and electricity form waste heat were evaluated. It is assumed that generated electricity could drive a conventional vapor compression chiller. The technologies were evaluated based on existing information available from the actual production process and the EFC technology. Several possibilities were identified: Organic Rankine Cycle (ORC), absorption chiller (AC), Kalina Cycle (KC) and thermoelectric generation (TG) based systems. Figure 1 shows different WHR technologies categorized by their energy vectors.

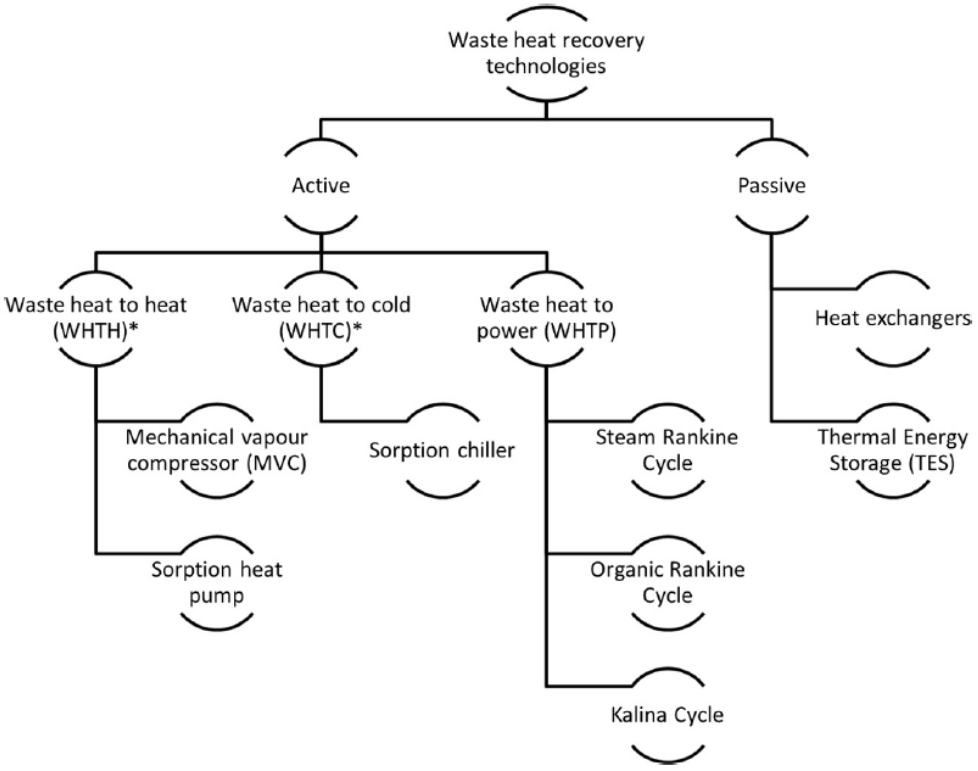

Figure 2: Categorization of WHR technologies. S. Brückner et al. [2].

4.1. Electro-mechanical technology options (Electricity generation)

Electro-mechanical technologies are activated through electrical input and alter the phase or other properties of a working fluid to pump heat.

Organic Rankine Cycle (ORC) occasionally referred to as the subcritical ORC, is currently used in various industrial low grade heat applications, such as binary geothermal power plants, solar thermal power systems, solar ORC-RO (reverse osmosis) desalination systems, Duplex-Rankine systems, ocean thermal energy conversion systems, waste heat recovery applications and biomass power plants, as described in detail by Tchanche et al. [4]. The temperature-entropy diagram of ORCs can be either bell-shaped or overhanging [5]. To give an example, the configuration of an ORC and its temperature-entropy chart are illustrated in Figure 3.

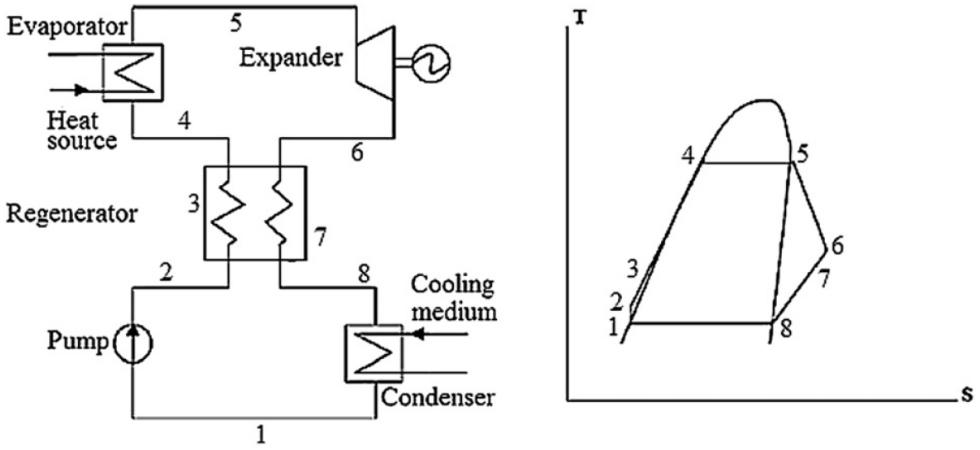

Figure 3: Organic Rankine Cycle (ORC) components scheme and Temperature-entropy chart Chan et al. [3].

Its working principles are similar to a Rankine cycle. The working fluid is pumped from low to high pressure with only little energy input (1-2). A regenerator can be added (optional) to improve the efficiency of the ORC, where the higher temperature fluid leaving the expander (6-7-8) can be used to preheat the lower temperature fluid (2-3-4) before it enters an evaporator.

After entering the evaporator, the liquid is heated at constant pressure by an external heat source and becomes a dry saturated vapor (4-5). The dry saturated vapor expands in the expander and generates power (5-6). This decreases the temperature and pressure of the vapor, which is then condensed at a constant temperature in a condenser to become saturated (8-1) before it is pumped to the evaporator.

While Rankine cycles usually operate at temperatures above 400°C, the ORC works effectively at lower temperatures, typically between 100°C and 400°C because in an ORC cycle:

- Evaporation takes place at lower pressure and temperature;
- Expansion ends in the vapor region, hence superheating is not required; and

- The smaller temperature difference between evaporation and condensation leads to a much smaller pressure drop ratio which allows the use of single stage turbines.

The recent work by Quoilin et al. [6] on six different kinds of working fluids, with evaporating temperature between 94°C and 143°C, reported that the efficiency of an ORC is generally between 5 and 9% (net electrical output over the actual amount of low grade heat transferred to the evaporator) while the overall efficiency is between 2 and 5% (net electrical output over the amount of low grade heat available, but which may not be completely transferred to the evaporator).

Kalina Cycle: The Kalina cycle is a thermodynamic cycle for converting thermal energy into mechanical power. The working fluid in this cycle is a mixture of at least two different fluids (typically water and ammonia). Ammonia has a lower boiling point compared to water. Hence, when the temperature of the mixture increases, the ammonia will boil first. Reversely, when the mixture is cooled, water will condense first. Unlike the Rankine cycle, where considerable heat energy is lost in the isothermal evaporation of water into steam, the binary mixture in the Kalina cycle vaporizes non-isothermally, resulting in better performance, presenting less irreversibility. Variable temperature boiling permits the working fluid to maintain a temperature closer to that of the combustion gases in the boiler. The use of a mixture as the working fluid allows manipulating pressure in the system by changing composition of the mixture.
The working principles of thermodynamic cycles that are mainly used for waste heat recovery such as the Organic Rankine Cycle and the Kalina cycle were also studied and it was determined that the Kalina cycle offers a better result when the recovered heat is the medium-high grade. However, the ORC was a competitor when the recovered heat was in the low-medium range, as it is explained in [7].

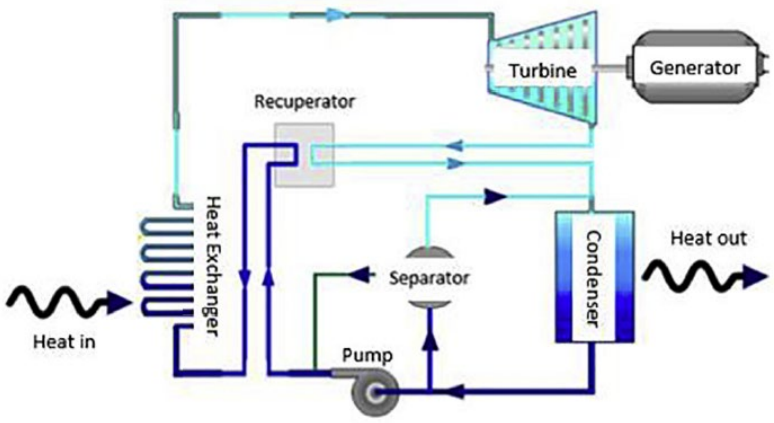

Figure 4: Configuration of a Kalina cycle consisting a Recuperator and Separator [7].

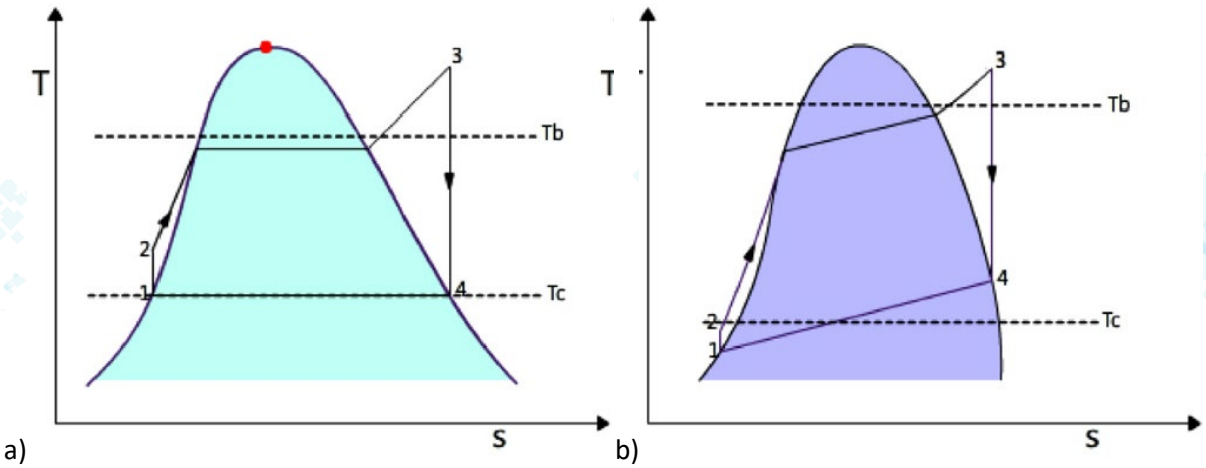

Figure 5: Comparison of T-S diagram of a) Rankine cycle and b) Kalina cycle [7].

Thermoelectric Refrigeration: Thermoelectric effect is achieved when there is a conversion from electrical energy to a temperature gradient. This effect was discovered by Peltier in 1834. This cooling system has no mechanical moving parts neither vibration. The cooling effect is reached when a direct current is passed through a semi-conductor material. The temperature of interconnecting n-type and p-type semiconductor material decreases so that heat is absorbed from the environment [8]. Moreover, the inverse effect in thermoelectric refrigeration is also produced. It is based on a temperature differential established between a cold and a hot source through a semiconductor material, where a voltage is generated. This voltage is called Seebeck voltage, and is proportional to the differential temperature. The effect is also used in thermocouples or thermo-resistances.

Finally, essentially the **duplex Stirling Heat Pump** consists in a Stirling engine driving a Stirling cycle heat pump. This comprises gas compression and expansion of a coolant, which oscillates between two chambers. Similar to the Stirling cycle the Vuilleumier is a closed cycle, where the working gas is kept inside the cylinders, heat is added to and removed from the cycle trough a heat exchanger allowing compression and expansion of gaseous working fluids [9].

4.2. Electrically Driven Heat Pumps

An Electrically Driven Heat Pump (EDHP) is a thermal machine that can lift the grade of a heat stream, consuming a smaller share electric energy. An EDHP consists of a mechanical compressor, an expansion valve, an evaporator and a condenser. Figure 5 shows the simplified working principle of a common EDHP; depicted is the pressure (p) versus the saturation temperature (T); Q_{EV} is the low temperature (T_{EV}) heat that is lifted to a higher temperature level (T_C) in the heat pump and (additionally to the driving energy Wel) released as Q_C. The refrigerant evaporates at a low temperature and pressure, taking up the heat from the low temperature heat source at the evaporator. The vapor is polytrophic compressed by means of mechanic energy to a higher pressure and therefore higher temperature. The

compressor is typically powered by electric energy. When the gaseous working fluid condenses it releases heat to the heat sink at the condenser at the higher temperature level.

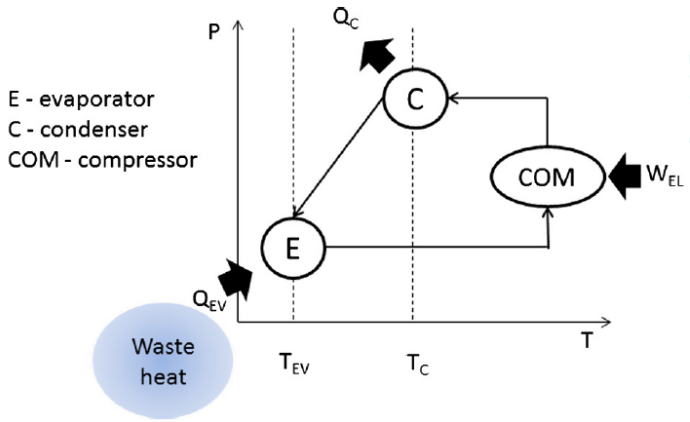

Figure 6: Simplified scheme of a electrically driven heat pump (HP) [2].

The external temperature levels determine which working fluids are appropriate for a certain application and which kind of compressor should be used. Here critical temperatures and vapor pressure curves of the refrigerant as well as pressure ratios of the compressors have to be considered besides other thermo-physical properties.

The maximum delivery temperature would be between 120 and 140°C due to material constraints caused by temperature and pressure. Common systems typically operate up to a maximum of 80°C. Due to the limited pressure ratio the lowest temperature at the low temperate heat source can be about -35°C for single stage machines operating with CO_2 as refrigerant, but this is strongly depending on condenser temperature. If the rejected heat at the condenser can be released below 0°C, heat at temperatures of about -50°C and below could be used at the evaporator.

The temperature lift (T1–T0) is limited by the compression ratio (the ratio of the pressure before and after compression) of the compressor and the temperature–pressure dependency of the chosen working fluid. Experimental set-ups demonstrate that the maximum possible lift is about 90 K; typically, these Machines are operating with a lift below 60 K. Common mechanically driven heat pump systems show an overall COP up to 4 during nominal operation, while mechanically driven refrigerators will reach an overall EER of about 3. With increasing temperature lift EER and COP decrease strongly. Therefore, the capacity of a given HP decreases with increasing temperature lift, too. This is mainly caused by losses increasing with the pressure ratio at the compressor.

4.2.1. Main parameters that the experimental set-up may test:

COP (Coefficient of Performance / Coefficient of energy efficiency in heating mode). Quotient between the heating power and the electrical power absorbed under specific temperature conditions and with the unit at full load.

EER (Energy Efficiency Ratio / Energy efficiency factor in cooling mode). Ratio between the cooling power and the electrical power absorbed under specific temperature conditions with the unit under full load.

SCOP (Seasonal Coefficient of Performance). Relationship between heating demand and electricity consumption, annually, in heating mode. Represents the overall performance of the unit throughout the designated heating season.

SEER (Seasonal Energy Efficiency Ratio). The overall energy efficiency factor of the unit, representative of the entire cooling season, calculated as the reference annual cooling demand divided by the annual electricity consumption for cooling. Basic concepts of the Heat Pump

SPF (Seasonal Performance Factor) Estimated seasonal mean yield factor. Factor that refers to the "net seasonal efficiency coefficient in active mode" (SCOPnet), in the case of electrically driven heat pumps and to the "net seasonal ratio of primary energy in active mode" (SPERnet) in the case of powered by thermal energy.

Equipment consumption when switched off, deactivated by thermostat or on standby. Operation of the equipment with partial loads (100%, 74%, 47%, and 21%)

4.2.2. Possible failures: Icing of Air/Water heat pumps

The evaporators on heat pumps using air as a heat source can freeze at low source temperatures depending on the humidity of the air. These devices therefore have to provide periodic defrost cycles in order to free the evaporator of ice. These usually work with a reversal of the normal process, temporarily delivering heat for defrosting from the heating circuit. The energy required for this process is considered when determining the COP and results in a reduced rating. During testing according to the standard, the device operates over a four-hour period, and depending on the number of defrosting cycles completed in this time, the COP is calculated across one or more cycles. As the ice build-up and the number of defrost cycles are heavily dependent on the humidity of the air, this parameter has also been specified for each temperature level. Typically freezing occurs at testing points below 7ºC and devices can normally be run ice free above 7ºC. The COP rating reduction through defrosting cycles is in the region of 0.3-1.0 depending on the efficiency of the defrosting algorithm employed.

4.2.3. Correction for the pumps and fans

A further aspect to be considered when determining the COP is the power consumption of circulation pumps and fans. Some devices have hydraulic circulation pumps integrated into their design, whilst others are delivered without a pump. If this was disregarded, devices with integral pumps would be at a disadvantage due to their higher consumption of electrical energy. In order to allow for this the standard includes a correction for the pump. The basis for this is the assumption that only the capacity necessary to overcome the device's internal pressure loss should be ascribed to the device itself. The correction is based on the measurement of the hydraulic capacity and on its conversion, using a virtual pump or fan efficiency factor, into an equivalent electrical input. This is then either added to the electrical energy consumption value or subtracted from it.

4.3. Thermally Driven Heat Pumps (Cooling generation through waste heat)

Advantages of thermally driven chillers compared to electrically driven vapour compression chillers include the following:

- Maintenance costs are lower as there are fewer moving parts. Moreover, high speeds for running compression systems shall induce vibrations and noise.
- If solar energy or wasted heat is used for driving the cycle, the operation costs are lower as electricity consumption is very low.
- Performance is higher in nominal conditions than at a partial load.
- The substances used are environmentally (water, lithium bromide). It is important to avoid brown-out situations, related to the peak of electricity demand. Several technologies driven by thermal energy exist.

A brief explanation of the most representative is described in the next paragraphs.

Absorption technology: An absorption machine has the same scheme blocks as the refrigerating machine. The only difference can be found on cold focus temperature and on the use of heat. In this case the cold focus may be outside environment, while the medium focus can be the heating demands of a building. The hot focus can be of the same type that in a case of a cooling machine. It is important to remark that the economic advantage of using sorption chillers is defined not only from the design of the chiller but also from the implementation in a solar cooling system. Low operating costs are achieved while maintaining desired operating conditions. Performance can be increased by improved control strategies which refer to the whole cycle, including thermal energy storage, solar loop, chilled water loop, environmental conditions and the chiller itself [10][11].

Adsorption technology: Adsorption cooling systems are also suitable in order to be considered part of the alternative cooling systems for a better energy management. This kind of systems are also capable to recover waste heat at low temperature levels. Therefore, very low quality energy can be used. At the same time, an adsorption cycle can be combined with cold production using thermo-chemical energy storage. This is a key point to be faced in new small capacity cooling systems. Many papers show relevant progress in the field of adsorption systems: [12][13]. New technical advances in solid sorption systems are expected in terms of developing new and thinner coatings of sorbent materials. This will allow sorption phenomena to be faster. An extended analysis can be found in [14].

On the other hand, there are several questions which have to be faced in adsorption systems such as: its poor heat transfer (low specific power, high capital cost) and low COP. This causes a high running cost concerning the design point of view. The low thermal conductivity is caused by the use of the adsorbent in grains. Therefore, implies that heat transfer depends on the contact points. Another problem to be addressed is its discontinuous operation that means unsteady output. Finally, it is important to notate that properties are not always well-known so that numerical simulation of adsorption systems is a new challenge to be faced. Concerning the basic process, one of the most important differences between absorption and adsorption is that in the first case exists a variation of the concentration of the solution that conveys the refrigerant which directly affect the thermo-physical properties. On the other hand, in adsorption system there is no variation of the composition of the fluid because the phenomena consist mainly in the affinity of a solid with a gas (e.g. water vapour) to be adhered on the surface in an exothermic process.

In next figure it can be observed the basic configuration of an adsorption cooling cycle. At initial state vessel 1 and vessel 2 are at ambient temperature and low pressure. Vessel 1 is high concentrated and vessel 2 is empty. Heat is being applied to vessel 1 so refrigerant begins to evaporate and being transported by pressure difference to vessel 2. Pressure increases at vessel 1. At vessel 2, once saturation pressure is achieved and temperature remains at ambient temperature, refrigerant condensates. Then pressure at vessel 2 is saturation pressure. On the other hand, at vessel 1 heat is continuously applied so that all refrigerant goes from vessel 1 to vessel 2. Adsorbent has to be cooled so heat has to be rejected in vessel 1 towards the ambient. During this process at vessel 1 temperature and pressure decreases and concentration increases because inside vessel 2 refrigerant begins to boil so that refrigerating effect appears. Once all the refrigerant has been transported from vessel 2 to vessel 1 the cycle is at the initial point again.

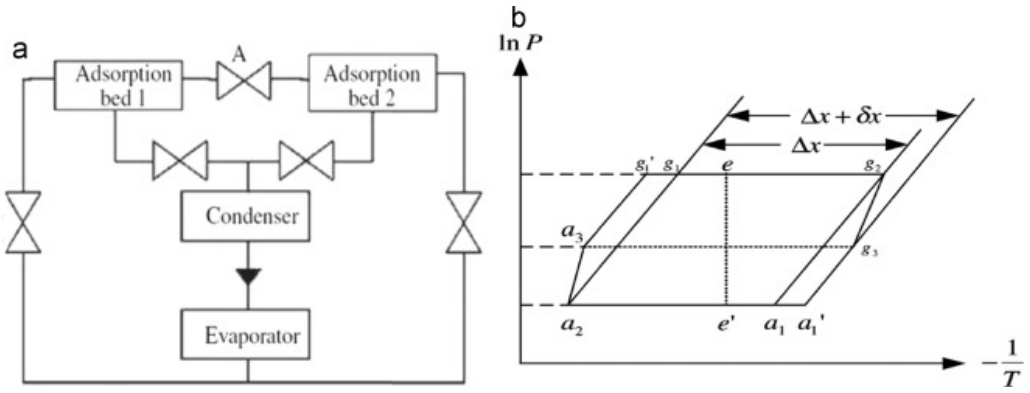

Figure 7: Adsorption components scheme and P-T chart.

Ejector Heat Pump: Ejection systems consist in accelerating and compressing a fluid by another which is pressurized by means of being thermally driven. In the ejector cycle, the refrigerant at low pressure (e.g. Water or other refrigerants) is driven by thermal energy, then the refrigerant is condensed, pumped and the kinetic energy transformed in pressure in the ejector. Figure 8 shows a schematic of the essential elements in an ejector system. Waste heat shall be used in order to convert water to super-heated steam. The ejector refrigeration cycle (as well as absorption cycle) requires very low amount of mechanical work.

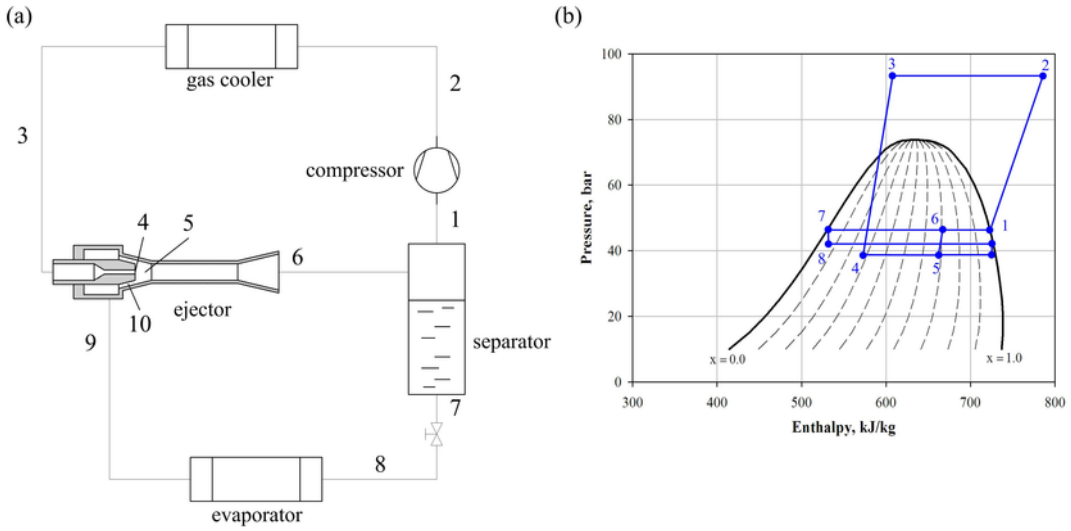

Figure 8: Ejector heat pump components scheme a) and P-h chart b).

4.4. Absorption cooling systems

The absorption chillers are only different from a traditional water chiller in the compression device. Instead of using a vapour compressor, which uses electricity as external power, an absorption chiller uses a thermochemical compressor, which uses heat as the main external power. Thermochemical compressors typically use a closed-loop circuit which uses a solution, in this case LiBr-H2O, which absorbs water vapour, produced at the evaporator, and transports it to the desorber, where the solution is heated up in order to remove the water that was captured in the solution, releasing water vapour.

Absorption fundamentals are based on the affinity between an absorbent and a refrigerant, which is driven by the difference of the liquid-vapour equilibrium conditions. If there is a mixture of an absorbent-refrigerant solution, the equilibrium pressure is lower than if there is a pure refrigerant, at the same temperature conditions. The absorbent is less volatile than the refrigerant. On the other hand, if a vessel which contains pure refrigerant and another vessel which contains a solution mixture that are conditioned to the same pressure conditions, the equilibrium temperature of the pure refrigerant is lower that when it is dissolved with the absorbent substance.

4.4.1. Single-effect cycle machine

Many contributions can be found in the scientific literature concerning the performance of a single-effect absorption cycle, e.g. [15][16]. The single effect cycle is composed by five heat exchangers (generator, absorber, solution heat exchanger, condenser and evaporator), a pump and two expansion valves. A description of the cycle can be found at Figure 9. Starting in the generator, the heat introduced warms the refrigerant-absorbent solution.

When the solution enters the generator, it is rich in refrigerant, but due to the heat introduced, part of the refrigerant evaporates, and the amount of solvent is reduced. This strong solution flows through a solution heat exchanger where is precooled and enters the absorber where it captures water vapour again. When the solution leaves the absorber, it has high concentration in refrigerant, it is preheated in the solution heat exchanger and reaches the generator again.

In the solution loop the pressure difference is achieved by means of a pump, which needs much less electrical power than a vapour compressor. The solution which has come to the absorber from the evaporator, becomes a weak solution. Finally, the released water vapour which flows out from the desorbed is condensed through the condenser and is injected back in the evaporator through an expansion valve, balancing the cycle.

Because the liquid-vapour mixture evaporates at the evaporator, this effect cools down the water that circulates through the secondary circuit and consequently decreasing its temperature.

Because the water vapour released at the desorbed is condensed, it releases this same energy to its surroundings, producing a wasted heat through the condenser.

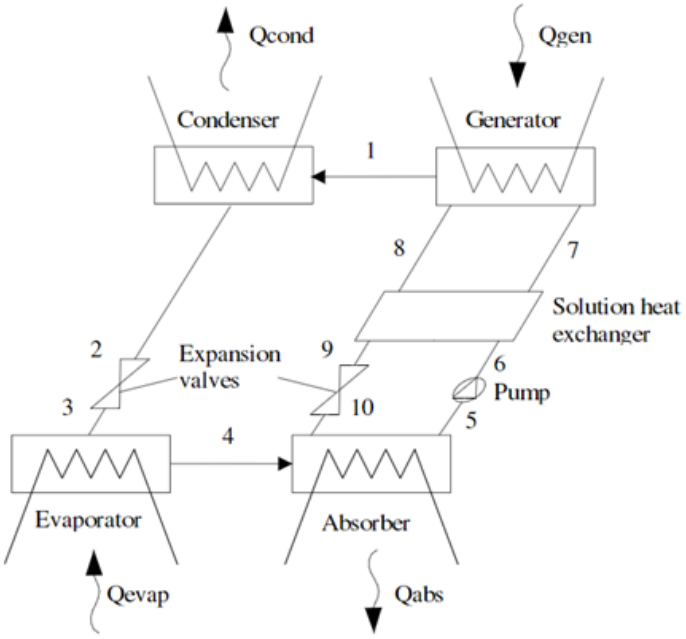

Figure 9: Single-effect LiBr-Water absorption heat pump.

4.4.2. Other cycle configurations

Several attempts are ongoing in order to realize systems to accelerate market penetration. Even though the aim of these attempts is the same, their approaches are variable: some research is ongoing to improve the COP of the absorption chiller, others are investigating the super positioning of single effect and double effect absorption cycles, others are focusing on producing high efficiency collectors with lower cost, also to take profit from different quality sources, etc. In that sense, the half-effect cycle chiller was developed by Kim and Infante-Ferreira [17][18] in order to take advantage from a **low temperature-driven absorption cycle**. It was theoretically investigated for the development of an air-cooled LiBr-Water absorption chiller to be combined with low-cost at solar collectors for solar air conditioning. To find ways to improve the coefficient of performance, Wang and Zheng [19] studied the one and a half-effect absorption cycle using LiBr-Water as working pair. The main idea was for a certain generation temperature, the adoption of the appropriate configuration of absorption cycle to use the heat of generation appropriately. Furthermore, there is a gap between the maximum desorber temperature from a single-effect absorption cycle and the minimum temperature needed to drive a double-effect absorption cycle.

Another approach to this temperature gap is the combined ejector-absorption refrigeration cycle. Simulation results showed that the COP of the cycle can be 30% higher than that of the conventional single-effect absorption refrigeration cycle [20].

Double-effect absorption cycles have a greater COP than single-effect but need higher temperatures to drive the chiller. Nevertheless, through solar energy it is also possible to run a double-effect chiller with high performances.

On the other hand**,** another absorption cycle called GAX (Generator Absorber Heat Exchanger Cycle) mainly based in NH3-H2O has also been attended by the academia and also by industry. Several studies can be found in [21][22][23][24].

Even though the next absorption configurations have not received the same attention than the previous ones, new developments are being done by research community. Next are itemized: i) Osmotic-membrane absorption [25][26], ii) Diffusion absorption refrigeration system [27][28][29], iii) Combined vapour absorption-compression cycle, iv) Sorption-resorption cycle, v) Self-circulation absorption system using LiBr-Water. Finally, at least it is important to remark the triple-effect cycle useful for large cooling capacity.

4.4.3. Working fluids of absorption cycles

In order to adapt the cooling demand requirements different working pairs can be used. As mentioned before, the main feature of the absorption machines is the capability to use low quality energy. Therefore, desirable properties clearly determine the suitability of the working pairs. Many basic conditions are required as itemized as follows: i) an absolute miscibility at the absorber pressure and temperature conditions and ii) total immiscibility at the desorbed regarding pressure and temperature. In the case of LiBr-H2O, mass fraction shall be lower than 70% in order to avoid crystallization.

Furthermore several properties shall be adequate to the working conditions: i) a high latent heat of the refrigerant, in order to reduce the total amount of circulating mass; ii) a refrigerant with low freezing temperature and much more volatile than the absorbent; iii) the operating conditions of the solution mixture should avoid crystallisation phenomena, otherwise it may induce an interruption of the cycle; iv)high chemical stability to avoid gases, solids or corrosion substances, v)low viscosity of the solution aiming to reduce the pumping electricity consumption; vi) low toxicity; vii) No flammability [30].

They can be used both in air conditioning systems (LiBrH2O) cycles, as they have better performance than NH3-H2O cycles at these temperatures, where temperatures are required to be 15-23 ºC, or for

cooling (NH3-H2Ocycles), as by far not found a better partner to sub-zero cold, LiBr-H2O cannot cool below 5ºC in practice), where temperatures are required between the range of -10 a +10 C.

Many reviews of working fluids of absorption cycles have been done where there are many refrigerant-absorbent working pairs which accomplish these conditions [31][32][33][34][35]. However, only two fluid pairs have been widely used in the market: LiBr-H2O and NH3-H2O. Nevertheless, there is an important e ort from the scientific community towards additives in order to enhance not only the performance of the cycle nut also to prevent from failures due to corrosion or freezing. The enhancement of both heat and mass transfer is a key aspect of absorption cooling technology. The inclusion of surfactants provides an increase in the surface tension gradients, which increases convection by boosting the Marangoni instability [36]. The use of advanced surfaces and vibrations provides extra mixing by increasing turbulence in the flow [37][38]. By all these means, the heat and mass transfer is enhanced in the absorber and therefore the capacity of the chiller is increased. On the other hand, the use of ionic liquids as working fluids are being attended by the scientific community due to several advantages they do not evaporate, its low toxicity, less corrosion, its capacity of dissolving CO2, non-flammability, stability at wide temperature range, less crystallization compared to conventional working fluids (LiBr-H2O and NH3-H2O). Nevertheless, the thermodynamic considerations must be taken into account in order to assure if an ionic fluid acts correctly to a determined refrigeration or cooling application. Other working fluids seem to be promising such as LiNO3 or the quaternary salt mixtures (LiBr, LiI, LiNO3, and LiCl). If internal storage is addressed, LiCl-H2O has an excellent storage capacity and efficiency but at high cost [39].

4.4.4. State of the art of Sorption players

Although commercial application of solar cooling is relatively new, the main progress of solar cooling techniques has been in the field of small capacity thermally driven sorption chillers.

In fact, numerous systems are installed due to many companies had been working in this field. Absorption and adsorption are the main dominant technologies used to cool. Significant companies that have an important role into the market are:

Absorption global players: Yazaki (Japan), Dalian Sanyo Refrigeration Co.Ltd./Panasonic (Japan), Trane Inc.(US), Entropie SAS (France), York International Corp.Market (US), Broad Air Conditioning Co Ltd. (China), Carrier Corporation (US), Finetec Century Corporation (South Korea), SolarNext (Germany), Ebara Refrigeration Equipment and Systems Co. Ltd (Japan), Thermax Ltd.(India), Johnson Controls (Japan), LG Machinery (USA), McQuay International (USA), Mitsubishi Heavy Industries Ltd.(Japan), Kawasaki (Japan), Dunham-Bush Holding Bhd (Malaysia), EAW GmbH (Germany), Shuangliang Eco-Energy Systems Co. Ltd. (China), Robur Corporation (USA), Pink (Austria), Econicsystems Innovative

Heizlosungen Gesmbh (Austria), Ago (Germany), FH Stuttgart (Germany), SolarFrost (Austria) , Aosol (Portugal), etc.

Adsorption: Nishiyodo Kuchou Manufacturing (Japan), Mayekawa (Mycom) (Japan), Sortech AG (Germany), SolabCool (Netherlands), SJTU (SWAC-10) (China), Invensor GmbH (Germany), GBU mbH (Germany), EcoMax (US).

Solid Dessicant cooling: Munters USA (US), Munters AB (Sweden), Seibu Giken (Japan), Earth Clean Thoku Co. Ltd. (Japan), Nichias (Japan), Amefrec Co. Ltd. (Japan), Panasonic Ecology Systems Co. Ltd. (Thailand), Mitsubishi Plastics Inc. (Japan), DRI (India), Klingenburg GmbH (Germany), ProFlute (Sweden), Bry-air (US), Rotor Source (US), Novel Air (USA), Dryer Air-handling Equipment Co. Ltd. (China), Sat Air Treatment Co. Ltd. (China), Munters Air Treatment Equipment Co. Ltd. (China), Wuxi Shamo Dehumidifying Equipment Co. Ltd (China), Wuxi Aobo Dehumidifying Equipment Co. Ltd (China), Hangzhou Dry Air Co. Ltd (China), Shanghai Hanfu Air Treatment Equipment Co. Ltd. (China), Guangzhou Huagongtai Dehumidication Equipment Co. Ltd.(China).

Liquid Dessicant cooling: L-DCS (Germany-Singapore), Kassel Universisty (Germany), Stuttgart (Germany), Queens University (Canada), University of South Australia (Australia), Technion Haifa (Israel), Florida (USA), Genius (US), Kathabar (USA), AIL Research Inc. (USA), Liquid-Dessicant Air Conditioner Menerga (Germany).

Thermo-mechanical chillers: AC-Sun (Denmark), Turboden (Italy), Ormat Technologies Inc. (US), LTi ADATURB GmbH (Germany).

Steam jet chillers/Ejectors: Fraunhofer Institute UMSICHT (Germany), AEE-Institute for Sustainable Technologies (Austria), University of Stellenbosch (South Africa), University of Nottingham (UK), Universitée Catholique de Louvain UCL (Belgium), Selcuk University-Alaeddin Campus (Turkey), National Taiwan University (Taiwan), The Australian National University (Australia).

5. WHRS-EFC system assessment

5.1. Waste Heat availability in silica industry

In the industrial silica production process, the precipitated silica must be dehydrated at the spray-dryers. For the dimensioning of the whole WHR system, the process from IQE has been taken as a reference. The dryers require an input of hot gas at 300 °C, to ensure a temperature range between 95 and 130 °C for drying process. For a production plant with a capacity to generate 26,600 $tSiO_2$/year, the dryer requires a hot gas mass flowrate of 55,500 kg/h at 300 °C. Considering an average outlet temperature from 95 to 130°C, the available thermal power supplied to the absorption chiller can range from 356.71 to 899.53 kW_{th}.

Table 1: Relevant information of the silica industry (provided by IQE).

Description	Value	Units
Brine		
Silica annual productivity (SiO_2)	26,600	t/year
Waste brine flowrate (containing Na^+ and SO_4^-)	210,000	m^3/year
$Na_2SO_4 \cdot 10H_2O$ brine concentration	66	kg/m^3
$Na_2SO_4 \cdot 10H_2O$ mass flowrate	13,860	t/year
Waste heat		
Hot gas mass flow rate	55,500	kg/h
Dryer gas inlet temperature	300	°C
Dryer gas outlet temperature range	95-130	°C
Available waste heat power (72°C as T return)	356.71-899.53	kW_{th}

5.2. Absorption Chiller selection and characteristics

The AC selected must allow the operation with the available waste heat and the EFC cooling demand.

The EFC needs to reach operating temperatures below zero. Thus, the refrigerant which accomplishes the EFC requirements is LiBr-Water cycles. Furthermore, alcohols must be considered, and some modifications focused, being a novel research line which only a few manufacturers are considering for their core business.

5.2.1. Basic scheme

The system to be simulated is a single-effect H_2O-LiBr absorption cycle. Figure 10 shows a schematic representation. For each component, overall balances of mass, species and energy have been

established under transient conditions. In order to close the system, momentum balance has been assumed for the two expansion valves.

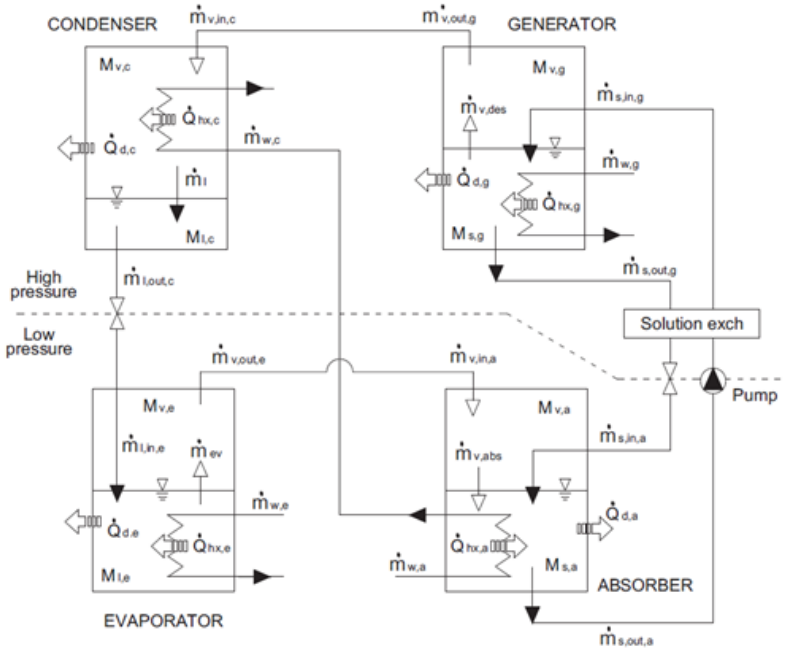

Figure 10. Schematic of the main components inside the absorption machine (white arrows: vapor, black arrows: liquid).

5.2.2. Technical characteristics

In order to achieve a -5°C chilled water impulsion temperature in an absorption machine fired with the lowest possible temperature, the machine selected is a single-stage LiBr/Water manufactured by Johnson Controls Ltd (previously York). To reach sub-zero temperatures, the thermal fluid has to be mixed with glycol (34%wt) and this requires the manufacturer to customize the commercial model that approaches the most this operating point. Due to these modifications, the performance curves of the machine are not available, and the only data available are simulations ad-hoc carried out by the manufacturer on demand. Table 2 shows the technical specifications of the selected device. To estimate its performance, the part load/COP curve from the commercial catalogue is taken as shown in Figure 10.

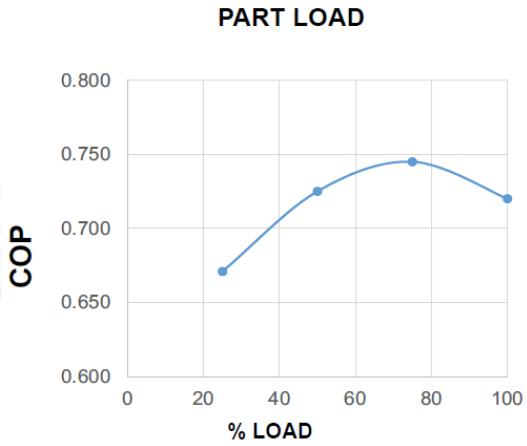

Figure 11: Nominal part load/COP chart of a YHAU series machine.

Figure 11 depicts the physical aspect of a YHAU unit, similar to the one chosen for the EFC.

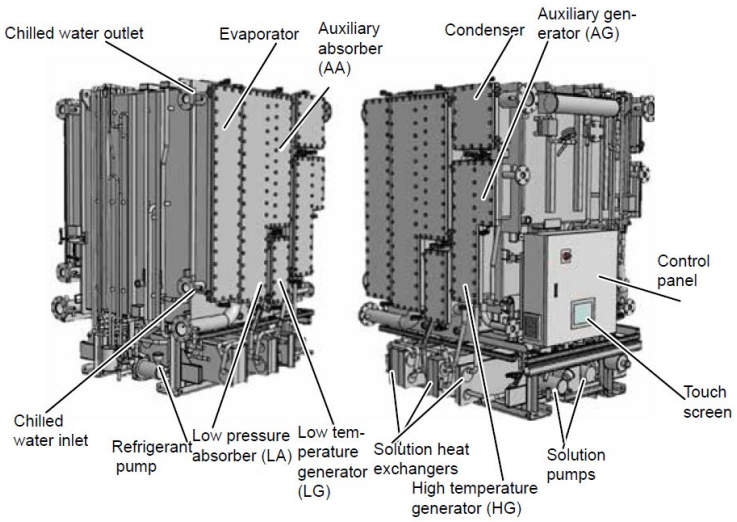

Figure 12: Graphical render of unit components of a York/Johnson Controls - YHAU series.

Table 2: Technical specifications for the YHAU-CL400 from Johnson & Controls S.L. modified to supply -5°C.

Project 2G AKM, Germany

14 Oct 2019

YORK (Wuxi) Air Conditioning and Refrigeration Co., Ltd.

S001-rev.0

Low Temp. Generate Absorption Chiller
Specification Sheet

Type		-	Low Temp. Generate Absorption Chiller
Model		-	YHAU-CL400EXSLL
Pressure Vessel Code		-	PED/SEP
Standard		-	GB, CE
Quantity		Unit	1
Cooling Capacity		kW	325
		USRT	(92)
COP		-	0.33
Chilled water	Fluid	-	34wt% Ethylene Glycol
	-Density	kg/m3	1,054
	-Viscosity	Pa·s	0.0057
	-Specific heat	kJ/kgK	3.58
	-Heat conductivity	kW/mK	0.00047
	Connection (inlet)	A	100
	Connection (outlet)	A	100
	Inlet temperature	°C	0.0
	Outlet temperature	°C	-5.0
	Flow volume	m3/h	62.1
	Pressure drop	kPa	103
	Pass	-	8
	Fouling factor	m2K/kW	0.0176
	Max. operating pressure	MPaG	0.8
Cooling water	Fluid	-	34wt% Ethylene Glycol
	Amount of heat	kW	1,313
	-Density	kg/m3	1,039
	-Viscosity	Pa·s	0.0018
	-Specific heat	kJ/kgK	3.68
	-Heat conductivity	kW/mK	0.00048
	Connection (inlet)	A	200
	Connection (outlet)	A	200
	Inlet temperature	°C	29.0
	Outlet temperature	°C	34.0
	Flow volume	m3/h	247
	Pressure drop	kPa	43
	Pass	-	3
	Fouling factor	m2K/kW	0.044
	Max. operating pressure	MPaG	0.8
Driving heat source	Fluid	-	Hot Water (fresh water)
	Amount of heat	kW	988
	Connection (inlet)	A	125
	Connection (outlet)	A	125
	Inlet temperature	°C	95
	Outlet temperature	°C	72
	Flow volume	m3/h	38.0
	Pressure drop	kPa	23
	Pass	-	6
	Fouling factor	m2K/kW	0.0176
	Max. operating pressure	MPaG	0.8
Power	Power supply	-	AC400V 50Hz 3Ph
	Electric capacity	kVA	approx. 21.0
	Power consumption	kW	approx. 17.0
Pump rated output	Intermediate Chilled Water Pump (P1)	kW	2.2
	Solution Circulation Pump (P2)	kW	3.0
	Solution Spray Pump (P3)	kW	2.2
	Solution Spray Pump (P4)	kW	2.2
	Refrigerant Spray Pump (P5)	kW	0.4
	Refrigerant Spray Pump (P6)	kW	0.4
	Purge Pump (AP)	kW	0.75
Weight	Max. shipping	ton	Approx. 13.5
	Operation	ton	Approx. 26.0
Outline dimension	Length	m	Approx. 6.3
	Width	m	Approx. 4.5
	Height	m	Approx. 3.6
Cold insulation area		m2	Approx. 44
Hot insulation area		m2	Approx. 22
Noise level		dB(A)	Approx. 85
Installation place		-	Indoor / non-hazardous

*There is a possibility that above table data is subject to variation with design progress.

*The chiller shall be split into two pieces during transportation and shall be re-assembled at site.

5.3. EFC model

The sodium sulphate recovery technology is the Eutectic Freeze Crystallisation (EFC) as it one of the main goals of the ZERO BRINE project. The main advantages of this technology are that it has lower energy requirements comparing with conventional Evaporation-Crystallisation (EC) systems due to the fact that the latent heat of ice formation (334 kJ/kg) is 6 times lower than the vaporisation one (2264 kJ/kg); and recovery of high purity.

To evaluate the performance of the Eutectic Free Crystallization technology in terms of mass flowrate of recovered salt and energy consumption, the analytical model developed by Eurecat in WP5 has been taken and adjusted to predict the behaviour of a batch reactor for Na_2SO_4.

5.3.1. Determining the eutectic point

The eutectic point is the temperature at which both ice and salt start crystalizing at the same time, shown in Figure 12.

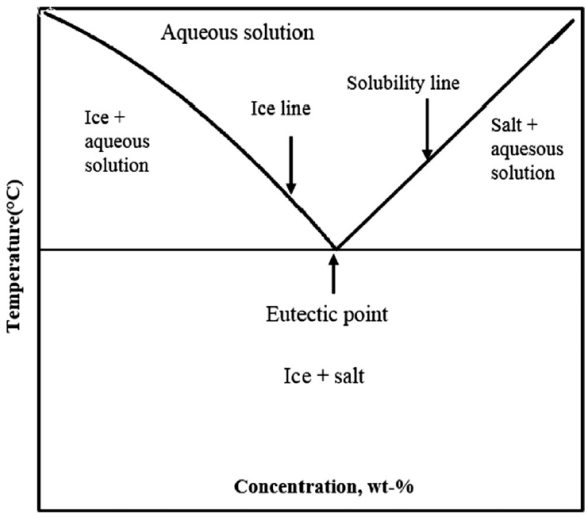

Figure 13: Phase diagram of a binary aqueous solution. [41]

Eutectic point for the stream to be treated by EFC (see Table 4) was determined at bench and pilot scale. In Deliverable 4.3 and 4.5, experimental results for EFC evaluation are described.

Table 3: Composition of the concentrate stream produced in membrane stage. This stream feed EFC (source D4.5).

Parameter	Unit	Value
pH		7.8
Conductivity	ms/cm	81.2
Al	µg/L	<10
Si	µg/L	54.3
Mn	µg/L	156
Fe	µg/L	146
Sr	µg/L	2930
Ba	µg/L	271
Na	mg/l	20488
SO_4^{2-}	mg/l	46155
Cl^-	mg/l	580

Sulphate concentration is 80-fold higher than chloride. Therefore, the eutectic point can be approximated to the Na_2SO_4 – Water binary composition. In Table 5 eutectic point for this solution is around to -1.3°C.

Table 4: Eutectic freeze points recorded (source D4.3).

Eutectic freeze point recorded (°C)				
Na_2SO_4 system (value from literature)	Na_2SO_4 – $NaHCO_3$ system	Na_2SO_4 – NaCl – $MgCl_2$ system	Synthetic RO concentrate	Synthetic concentrated RO concentrate
-1.27	-1.34	-1.36	-1.36	-1.49

5.3.2. Operating regime of the EFC model

To evaluate the EFC technology, a simulation is run for the concentrate stream with the characteristics from IQE. This stream has a concentration of 66gNa_2SO_4/m^3, and its flow temperature is estimated at 25°C. To reach the eutectic point, the stream must be cooled down as indicated in Figure 14. While going from starting point (point 1) to saturation limit (point 2) it consumes sensible heat, and no salt appears. When saturation limit is reached as it keeps cooling down, salt starts crystallizing and precipitates, and therefore concentration diminishes moving along the solubility line until eutectic point is reached (point 3). This salt is crystallized without generating ice consuming only sensible heat and appears pure if its solubility line does not cross with other solved compounds. When eutectic point is reached, the simultaneous crystallization of both salt and ice starts by keeping conditions slightly below eutectic point. During this stage, latent heat to maintain that operation is consumed.

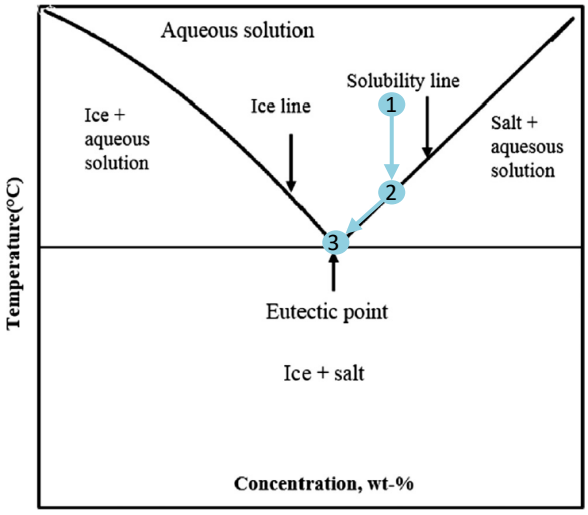

Figure 14. Feed conditions and approach to the eutectic point. Starting point (1), saturation limit (2) and eutectic point (3).

The sensible heat demand from 25 to -1.3°C is 108.36 kJ/kg and the latent heat demand is 334 kJ/kg.

5.3.3. Presentation of the model

In Task 5.3 of the ZERO BRINE project, Eurecat developed an analytical model of the EFC technology. It can be found in detail in deliverable D5.2. The model is used assuming the following hypothesis:

- The crystallization vessel is equipped with agitation blades operating at a high rotation speed. The addition of agitation of ice crystals improves significantly the yield of salt crystals since they are not encapsulated in the ice crystals, thus, improving the purity of recovered ice as well [40].
- The agitation acts as an ice scrapper as well avoiding the scaling of the vessel walls to grow thicker than 1mm.
- Both ice and salt crystallize simultaneously and grow at the same rate.
- Perfect mixing: temperature and concentration are uniform everywhere within the vessel.
- Crystals are considered to be spherical in shape
- There are no heat losses in the whole system

The model has been implemented as a Matlab function with the input/output variables shown in Table 6. The model can calculate the salt production and energy consumption of the crystallizer as a function of the starting mass fraction or salt concentration, and sub-cooling temperature.

Table 5: Structure of the EFC model function.

[output] = EFC_model_function(input)			
	Description	**Name**	**Units**
Input variables	Mass fraction	y_i	%
	Chilled water inlet Temperature	T_{CHW_in}	°C
	Size of the vessel (height and radius)	L_v, r_i	m
	Coolant inlet temperature	T_C	°C
	Operating temperature	T_L	°C
	Stream concentration	C	kg/m^3
Output variables	Scaling thickness (vector as a function of time)	γ_i	m
	Crystal volume fraction (vector as a function of time)	V_{of} / Φ	%
	Crystallised mass (vector as a function of time)	M_{of}	kg
	Consumed cooling heat (vector as a function of time)	Q	W
	Time vector	t	s

The equation to calculate the Crystal Volume Fraction (V_{of}) is defined by:

$$\frac{1}{\Phi} = \frac{1}{\alpha_1 (C - C_{eq})^3 t^4 \exp\left(\frac{\alpha_2}{T}\right)} + 1$$

And the ice scaling thickness (γ) is determined by:

$$\gamma = \frac{\alpha_3 \Phi V_v}{S_v}$$

Where C is the concentration of salt in the solution, C_{eq} is the concentration of the solution at the eutectic point, t is the time, T is the temperature of the solution and Φ is the volume fraction of crystals. In the second equation V_v is the volume of liquid contained in the vessel and S_V is the surface of the vessel wall where the ice scaling will deposit. Coefficients α_1, α_2, and α_3 are determined by the nucleation rate and the growth rate of crystals of both ice and salt. These coefficients give the time depending response of the model according to the crystallization kinetics and need to be adjusted by using real experimental data of the ice crystallisation and salt mass precipitation along time.

5.3.4. Adjusting model coefficients

Coefficients α_1, α_2, and α_3 have been manually adjusted to the experimental data presented by Nathoo et al. (2009)[42], where an EFC treatment protocol is set up for the treatment of multi-component hypersaline brines at a major scale of 100 m^3/day. From this document, the yields of salt and ice per time unit can be used to characterize the crystallization kinetics of a solution mainly made of Na_2SO_4, but also with a smaller presence of NaCl and other minor ions. The setup consists of a batch operation crystallizer with agitation impeller, the same topology as the one assumed in the model from Eurecat.

The experimental setup used a brine from the reverse osmosis retentate from typical mine water, with the following composition:

Table 6: Composition of experimental Brine (Nathoo et al.,2009)[42].

Ions	Concentration [mg/L]
Cl^-	2260
SO_4^{2-}	7440
Na^+	5027

Composition from Table 6 means a concentration of C = 12.47 kg/m^3 of Na_2SO_4 and at 100 m^3/day, which represent 4.6 m^3/h, this is a concentrated mass flowrate of 57.35 kg/h. The yields of operating 24 h and processing a volume of 100 m^3 at -5°C employing an electrical compression chiller are presented in Table 7.

Table 7: EFC experimental yields (Nathoo et al.,2009)[42].

	Value
$Na_2SO_4.10H_2O$ produced [kg/h]	104
$NaCl.2H_2O$ produced [kg/h]	-
Ice produced [kg/h]	3912
Cooling duty [kW]	504

The ice produced after 1 hour of operation is 3912 kg/h of a 4.6 m^3/h flowrate @ -5°C and a density of 917.5 kg/m^3, and this is a crystallized volume of Φ=92.69%. The ideal recovered salt amount, according to brine concentration should be:

$$m = \Phi \cdot C \cdot V_v = 92.69\% \cdot 12.47 \frac{kg}{m^3} \cdot 4.6\, m^3 = 53.13\, kg\, Na_2SO_4$$

From the molar weight it can be calculated the ideal yields of Glauber's salt. The molar weight for Na_2SO_4 pure is 142.1 g/mol and for water it is 18 g/mol. The composition of the Glauber's salt is $Na_2SO_4 \cdot 10H_2O$. The precipitated mols of pure Na_2SO_4 are:

$$n = \frac{53130\ g}{142{,}1\left(\frac{g}{mol}\right)} = 374.07\ mol Na_2SO_4$$

And therefore, the mass of water is:

$$m\ H_2O = 10 \cdot n \cdot 18\frac{g}{mol} = 10 \cdot 374.07 mol \cdot 18\frac{g}{mol} = 67.33\ kg\ H_2O$$

The ideal mass of Glauber's salt is the sum of both fractions and it is 120.49 kg. The real yield of Glauber's salt is 104 kg/h. This means a recovery ratio of 86.31% of the salt. The salt recovery reduction can be attributed to salt crystals encapsulated in the ice crystals when these are being formed. This ratio can be increased using agitation in the vessel [40].

According to these results, coefficients α_1 and α_2 can be manually adjusted to adjusts model results to experimental data where it takes 1h to reach a 92.69% of crystallized volume. The mass of crystallized salt is equivalent to the mass precipitated from the crystallized ice volume. Regarding the ice scaling on the vessel walls surface, the ice scrapper does not allow it to grow thicker than 1mm, and thus it is considered to be constant.

Table 8: Adjusted values for EFC model coefficients.

Coefficient	Value
α_1	3.9e-11
α_2	1e-1
α_3	-
Rr (Recovery rate)	86.31%

Figure 14 presents the evolution in time of the crystallization process showing the volume crystallized volume fraction and the crystallized salt mass.

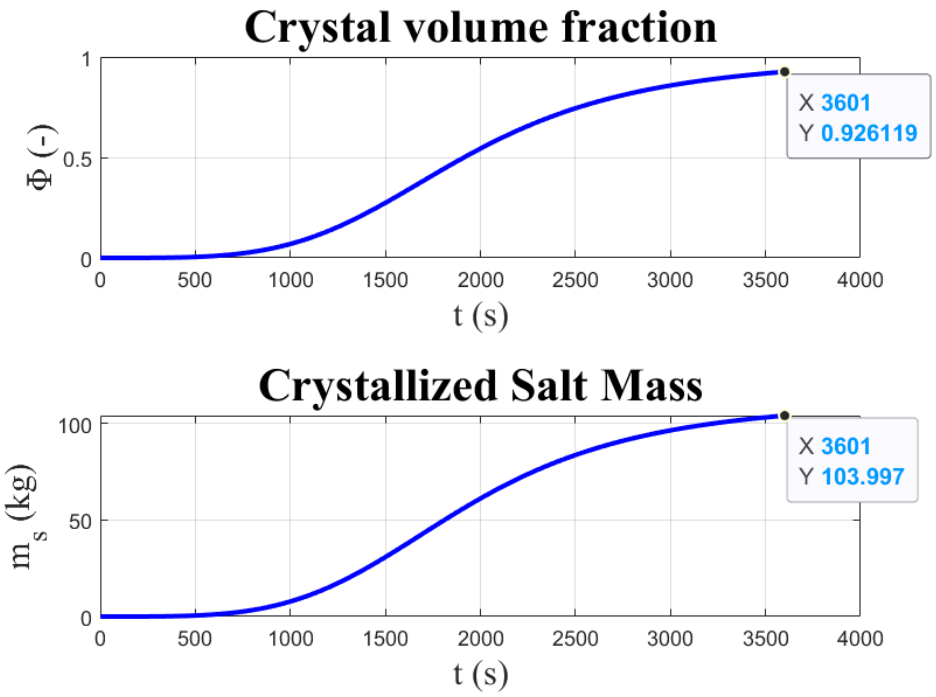

Figure 15: Result of the model simulation after adjustment. It shows the evolution of crystal volume fraction (V_{of}) and crystallized salt mass.

After 1 hour of operation the 92.61% of the volume has crystalized and 104 kg of salt have crystalized.

5.4. WHRS-EFC solution

In this section is proposed the whole system to recover Na_2SO_4 and the waste heat. The flow chart (Figure 16) shows the configuration of the solution. The hot gas enters the dryers to dry the silica, and leaves them at a temperature between 95 and 130 °C with an average value of 110°C. The waste heat is recovered with a gas/liquid heat exchanger and it feeds the absorber of the absorption chiller. The absorption chiller also has a secondary circuit of cooling water that needs to be dissipated outdoors with an automatically regulated cooling tower to keep the outlet temperature below 34°C. The cooling generated in the chiller is fed into the EFC at -5°C allowing to recover the Glauber's salt from the rest of the waste brine.

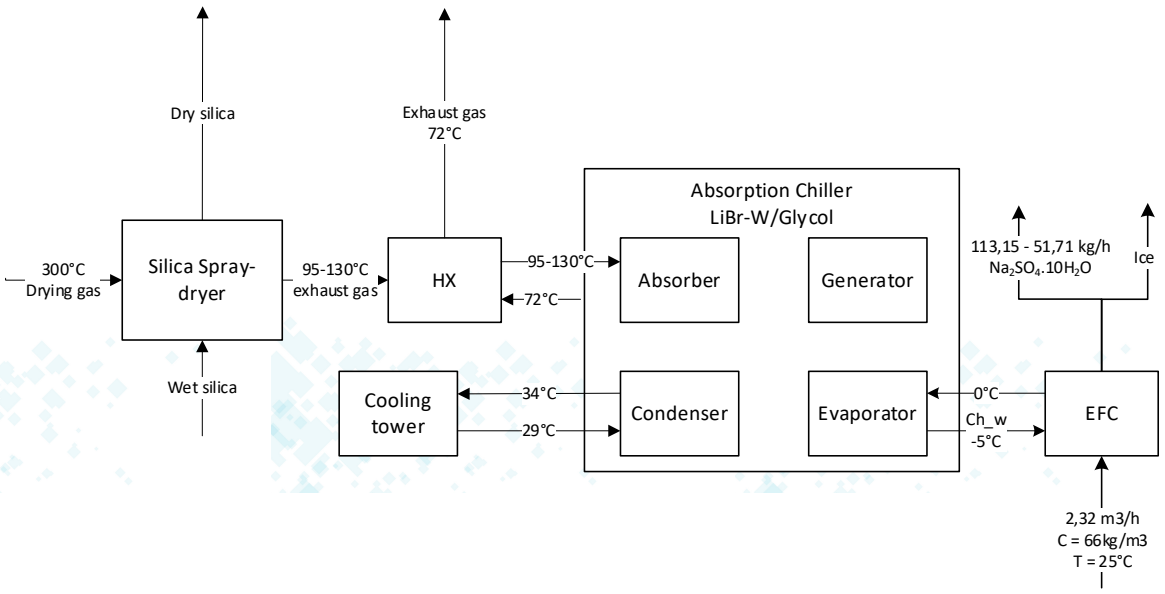

Figure 16: Scheme of the Waste Heat and Glauber's salt recovery system proposed for the silica industry.

The waste heat available from the gas spray-dryer ranges from 356.71 to 899.53 kW_{th} corresponding to 95 to 130°C. Using the single effect absorption chiller from York modified to reach sub-zero temperatures at -5°C, the nominal COP drops from 0.67 to 0.33. Nevertheless, operating at partial loads, the load vs. COP chart for standard conditions (chilled water supply T = 7°C) is assumed, and thus for an 83.96% to 33.19% partial load, the COP decreases to 0.3212 and 0.3249 respectively, which means a useful cooling power of 274.48 kW_{th} and 110 kW_{th}.

For the maximum cooling power, the maximum stream that can be processed in the EFC is 2.14 m^3/h, that supposes a sensible cooling power of 66.51 kW, and a latent heat power of 206.26 kW that account for a total power of 273.26 kW_{th}. In the next section results are exposed in further detail.

5.4.1. Performance assessment

The time profile of the outlet gas temperature from the dryer was undefined, and therefore, it was difficult to estimate the amount of waste heat available. The maximum temperature is 130°C and the minimum is 95°C. To calculate the performance of the recovery solution it was considered the average temperature of 110°C.

The available cooling power from the absorption chiller (AC) was determined from the equipment specification as a function of the partial load ratio (PRL) at which it works. The AC reaching -5°C implies modifications and the use of a water-glycol solution. The variation of the COP with the PLR was not available for this equipment because it is a variation of the commercial version. As an approximation, the PRL-COP chart from the YHAU series (Figure 10) was taken to determine the COP decrease due to PLR. Finally, there was applied a global efficiency parameter of 95% that includes the efficiency of the heat transmission from the dryer flue gases to the cooling output of the AC.

The mass flowrate of Na_2SO_4 brine was determined as a function of the cooling capacity of the AC. The cooling demand was calculated with sensible and latent specific heat for reducing the brine flow from 25°C to -5°C and freezing it.

Finally, the production of the EFC reactor was estimated from the results of the model. For one hour of operation, the crystalized volume is 92.61%, the precipitated salt mass is equivalent to the concentration of that volume and considering a recovery ratio of 86.31%.

The electricity cost was taken from the average industrial supply of the Spanish electric grid of 0.08 €/kWh. The operation of the whole WHRS-EFC was evaluated for one year of operation.

Table 9 exposes the results of energy consumption, yields, operating temperatures and mass flowrates and operation expenses.

Table 9. Results of the WHRS-EFC proposed solution evaluated for one year operation.

EFC flowrate	Max.	Avg.	Min.	
WH				
T out gas	130	110	95	ºC
T exh gas	72	72	72	ºC
m_gas	55500	55500	55500	kg/h
m_gas	15,42	15,42	15,42	kg/s
cp_aire	1,006	1,006	1,006	kJ/kg·K
Pth	**899.53**	**589.35**	**356.71**	**kW_th**
m_EFC	**18000**	**11850**	**7100**	**m3/any**
h_year	8400	8400	8400	h/year
m_EFC	5.95E-04	3.92E-04	2.35E-04	m3/s
Cooling Power				
P sensible				
Ti	25	25	25	ºC
To	-1.3	-1.3	-1.3	ºC
DT	26.3	26,3	26.3	ºC
m	5.95E-04	3.92E-04	2.35E-04	m3/s
ro	1037.8	1037.8	1037.8	kg/m3
cp	4.12	4.12	4.12	kJ/kg·K
Q	66.94	44.07	26.40	kW
P latent				
Hl	334	335	335	kJ/kg
QL	206.32	136.24	81.63	kW
P total	273.26	180.30	108.03	kW
Absorption Chiller (AC)				
COP_nom	0.33	0.33	0.33	
%Capacity	83.96%	55.40%	33.19%	
D_COP (chart)	-0.0088	-0.0071	-0.0051	
COP_part	0.3212	0.3229	0.3249	
Pth_cool	288.93	190.30	115.90	kW_th
n_global	95%	95%	95%	
P useful	**274.48**	**180.79**	**110.10**	**kW**

Continuation of 10.

EFC flowrate	Max.	Avg.	Min.	
EFC				
prod	92.69%	92.69%	92.69%	voc
v_ice	1.986	1.308	0.783	m3/h
Concentration	66	67	66	kg/m3
Recovery Ratio	86.31%	86.31%	86.31%	
m_salt	113.15	87.61	51.71	kg/h
m_salt	**950,458.90**	**735,912.26**	**434,345.34**	**kg/year**
Economic and energy costs				
Specific energy	2.426	2.064	2.129	kWh/kg
LCOE	0.00752	0.00752	0.00752	€/kWh
Production cost	0.018	0.016	0.016	€/kg

The production of 1 kg of Glauber's salt obtained was 2.064 kWh/kg, and it costs 0.016 €/kg. The total mass of Glauber's salt produced was 735,912.26 kg/year. Considering that the mass flowrate of Glauber's salt contained in the brine is 13,860 t/year (from Table 1), the recovered salt with EFC technology is 5.3% of the possible recovered salt.

5.4.2. Economic and environmental assessment

To assess the economic feasibility of the solution, the capital and operation costs were estimated and the payback period was calculated.

The operation expenses (OPEX) are based on the electric energy consumption of the absorption chiller. The levelized cost of energy was calculated (LCOE) as well, as the cost to produce the cooling power for the EFC. Finally, the carbon dioxide emissions were also calculated.

Table 10. OPEX of the Absorption Chiller (AC) and calculation of Levelized Cost of Energy (LCOE).

OPEX		
AC		
Pel	17.00	kWel
h_year	8400.00	h/year
E elec	142.800.00	kWh/year
E cooling	1,518,598.60	kWh/year
Electric specific cost	0.08	€/kWh
Electric cost	**11,424.00**	**€/year**
CO_2 emission*	**46,267.20**	**kg CO_2/year**
LCOE	**0.0267**	**€/kWh**
(*) SimaPro Vdeveloper 8.520 (BBDD EcoInvent). Methodology Recipe 2016 Midpoint (H). Emission equivalence: 1MWh = 324 KgCO2eq (Medium-voltage Spanish Energetic Mix)		

For the estimation of the capital expenses (CAPEX), the manufacturer offered a cost of the AC of 325,000 €, including the transport. The cost of the cooling tower, with a capacity of 1.3 MW, is estimated as 100,000 € from commercial catalogues available in the market. The cost of the EFC reactor is uncertain, thus it is estimated as a high quality chemical reactor of 3 m^3 as 20,000 €. The auxiliary equipment and installation costs are considered as 10% of the AC cost.

Table 11. CAPEX of the whole WHRS-EFC system.

CAPEX			
AC cost		€	325,000.00
Cooling Tower		€	100,000.00
EFC reactor		€	20,000.00
Auxiliary equipment (10%)		€	32,500.00
TOTAL		**€**	**477,500.00**

For the economic feasibility, the cashflow for the following years after the implementation is calculated to obtain the payback of the investment.

As incomes, there are considered:

- Energy cost savings. The electrical energy consumption of the AC is much lower than would be in a VC conventional chiller (from Table 13). This difference is accounted as income for the payback.

Table 12. Economic and CO_2 emissions savings of the AC operation compared to a VC conventional chiller.

Savings		
VC-Chiller		
Pcool	180.79	kWth
COP	3	
Pel	60.26	kWel
h_year	8400.00	h/year
E cooling	1,518,598.60	kWh/year
E elec	506,199.53	kWh/year
Electric specific cost	0.08	€/kWh
Electric cost	40,495.96	€/year
CO_2 emission	164,008.65	kg CO2/year
AC		
Pel	17	kWel
h_year	8400	h/year
E elec	142,800	kWh/year
Electric specific cost	0.08	€/kWh
Electric cost	11,424	€/year
CO_2 emission	46,267.20	kg CO2/year
Electric energy savings	**363,399.53**	**kWh/year**
Electric energy savings	**71,78%**	
Economic savings	**29,071.96**	**€/year**
CO_2 emission savings	**117,741.45**	**kg CO2/year**
CO_2 emission savings	**71,78%**	
LCOE	**0.0267**	**€/kWh**

- Recovered salt revenues. Taking as reference the average market price for the Glauber's salt as 0.08 €/kg, it accounts for 98,860 €/year, as shown in Table 14.

Table 13. Revenues for selling recovered salt.

Salt production	1,235,743.08	kg/year
Salt price	0.080 €	€/kg
Salt revenues	98,859.45	€/year

As expenses, it has been considered the operation and maintenance costs (O&M) as 15% of the energy savings. The discount rate of the money value has been taken at 2%.

Table 14. Payback of the WHRS-EFC solution.

Discount rate		2%				
Year	0	1	2	3	4	5
Investment	-477,500 €	0.00	0.00	0.00	0.00	0.00
Energy savings		29071.96	29071.96	29071.96	29071.96	29071.96
O&M costs (15%)		-4360.79	-4360.79	-4360.79	-4360.79	-4360.79
Recovered salt revenues		98859.45	98859.45	98859.45	98859.45	98859.45
Cashflow	-477,500 €	121147.66	118772.22	116443.35	114160.15	111921.71
NPV	**-477,500 €**	**-356,352 €**	**-237,580 €**	**-121,137 €**	**-6,977 €**	**104,945 €**

For the described incomes and expenses the WHRS-EFC solution has a payback period of 5 years, when its net present value (NPV) of the investment becomes 104,945 €.

6. Conclusions

The conclusions of this study are the following.

- The waste heat available at silica industry is located in the gas-dryer. The outlet exhaust gas temperature ranges from 95 to 130°C.
- For the waste heat temperatures mentioned above, from all the waste heat recovery (WHR) technologies assessed, the most suitable one resulted to be the absorption chiller (AC). It can take benefit from the waste temperatures below 100°C, and at the same time can supply cooling power at sub-zero temperatures (-5°C).
- The application of the proposed solution presents an economic investment payback of 5 years.
- The mathematical model of the EFC was adjusted to experimental data from scientific literature. A further work adjusting the parameters to experimental data from the ZERO BRINE project needs to be done.
- In this study some hypothesis were considered, such as the ones implied in the EFC analytical model to calculate salt yields and the calibration of the model with literature data. Another hypothesis made is that the EFC can be escalated to a capacity of hundreds of kW. Nevertheless, a careful design must be carried out for this reactor in order the guarantee the cooling heat transfer, the agitation to all the vessel volume and the batch operation mode.
- The use of recovered waste heat with an absorption chiller to supply the cooling energy to the EFC supposes energy saving of 71.78% and the same amount of CO_2 emissions reduction.

7. References

[1] BREF LVIC - Best Available Techniques for the Manufacture of Large Volume Inorganic Chemicals – Solids and Others industry (August 2007).

[2] S. Brückner, S. Liu, L. Miró, M. Radspieler, L. Cabeza, E. Lävemann. Industrial waste heat recovery technologies: An economic analysis of heat transformation technologies. Applied Energy, 151:157-167, 2015

[3] Chan, C. W., J. Ling-Chin, and A. P. Roskilly. "A review of chemical heat pumps, thermodynamic cycles and thermal energy storage technologies for low grade heat utilisation." Applied thermal engineering 50.1 (2013): 1257-1273.

[4] B.F. Tchanche, Gr. Lambrinos, A. Frangoudakis, G. Papadakis, Low grade heat conversion into power using organic Rankine cycles e a review of various applications, Renewable and Sustainable Energy Reviews 15 (2011) 3963-3979.

[5] B. Saleh, G. Koglbauer, M. Wendland, J. Fischer, Working fluids for low temperature organic Rankine cycles, Energy 32 (2007) 1210-1221.

[6] S. Quoilin, S. Declaye, D. Tchanche, V. Lemort, Thermo-economic optimization of waste heat recovery organic Rankine cycles, Applied Thermal Engineering 31 (2011) 2885-2893.

[7] Jouhara, Hussam, et al. "Waste heat recovery technologies and applications." Thermal Science and Engineering Progress 6 (2018): 268-289.

[8] SB. Riffat and Xiaoli Ma. Thermoelectrics: a review of present and potential applications. Applied Thermal Engineering, 23:913–935, 2003. [42] GD. Mahan. Multilayer Thermionic Refrigeration. Phys. Lett. A, 76(4362), 1994.

[9] P. Bansal, E. Vineyard, and O. Abdelaziz. Status of not-in-kind refrigeration technologies for household space conditioning, water heating and food refrigeration. International Journal of Sustainable Built Environment, 1:85– 101, 2012.

[10] J. Castro, A. Oliva, C. D. Pérez-Segarra, and J. Cadafalch. Evaluation of a Small Capacity, Hot Water Driven, Air-Cooled H2O-LiBr Absorption Machine. International Journal of Heat Ventilation Air Conditioning and Refrigeration Research, 13(1):59–75, 2007.

[11] GA. Florides, SA. Kalogirou, SA. Tassou, and LC. Wrobel. Modelling, simulation and warming impact assessment of a domestic-size absorption solar cooling system. Applied Thermal Engineering, 22:1313–1325, 2002.

[12] F. Agyenim, I. Knight, and M. Rhodes. Design and experimental testing of the performance of an outdoor LiBr − H2O solar thermal absorption cooling system with a cold store. Solar Energy, 84:735–744, 2010.

[13] M. Izquierdo, R. Lizarte, J. D. Marcos, and G. Gutiérrez. Air Conditioning Using an Air-Cooled Single Effect Lithium Bromide Absorption Chiller: Results of a Trial Conducted in Madrid in August 2005. Applied Thermal Engineering, 28(8-9):1074–1081, 2008.

[14] F. Asdrubali and S. Grignaffini. Experimental evaluation of the performances of a H2O − LiBr absorption refrigerator under different service conditions. International Journal of Refrigeration, 28:489–497, 2005.

[15] R. Lizarte, M. Izquierdo, JD Marcos, and E. Palacios. Experimental comparison of two solar-driven air-cooled LiBr/H2O absorption chillers: Indirect versus direct air-cooled system. Energy and Buildings, 62:323–334, 2013.

[16] D.S. Kim and C.H.M. Machielsen. Comparative study on water and air-cooled solar absorption cooling systems. Technical report, Delft University of Technology, Delft, The Netherlands, 2002.

[17] D. S. Kim and C. A. Infante Ferreira. Air-Cooled Solar Absorption Air Conditioning. Technical report, Faculty of Design, Construction and Production, Mechanical Engineering and Marine Technology, 2005.

[18] D. S. Kim and I. Ferreira. Air cooled LiBr water absorption chillers for solar air conditioning in extremely hot weathers. Energy Conversion Management, 50(2009):1018–1025, 2007.

[19] J. Wang and D. Zheng. Performance of one and a half-effect absorption cooling cycle of H2O/LiBr system. Energy Conversion Management, 50:3087–3095, 2009.

[20] D. Hong, G. Chen, L. Tang, and Y. He. A novel ejector-absorption combined refrigeration cycle. International Journal of Refrigeration, 34:1596–1603, 2011.

[21] M. Izquierdo, JD. Marcos, ME. Palacios, and A. Gonzalez Gil. Experimental evaluation of a low-powered direct air-cooled double-effect LiBr − H2O absorption prototype. Energy-The International Journal, 37:737–748, 2012.

[22] M. Izquierdo, A. González-Gil, and E. Palacios. Solar-powered single-and double effect directly air-cooled LiBr-Water absorption prototype built as single unit. Applied Energy, 130:7–19, 2014.

[23] S. Garimella, R.N. Christensen, and D. Lacy. Performance evaluation of a generator-absorber heat-exchange heat pump. Applied Thermal Engineering, 16(7):591–604, 1995.

[24] M.D. Staicovici. Polybranched regenerative gax cooling cycles. International Journal of Refrigeration, 18(5):318–329, 1995.

[25] H.M. Sabir, R. Chretienneau, and Y.B.M. ElHag. Analytical study of a novel gax heat driven refrigeration cycle. Applied Thermal Engineering, 24:2083– 2099, 2004.

[26] C.P. Jawahar and R. Saravanan. Generator absorber heat exchange based absorption cycle—a review. Renewable and Sustainable Energy Reviews, 14:2372–2382, 2010.

[27] J.M. Rodríguez-Muñoz, J.L. and Belman-Flores. Review of diffusion–absorption refrigeration technologies. Renewable and Sustainable Energy Reviews, 30:145– 153, 2014.

[28] Z. Sayadi, N. Ben Thameur, M. Bourouis, and A. Bellagi. Performance optimization of solar driven small-cooled absorption–diffusion chiller working with light hydrocarbons. Energy Conversion and Management, 74:299–307, 2013.

[29] A. Yildiz and M.A. Ersöz. Energy and exergy analyses of the diffusion absorption refrigeration system. Energy, 60:407–415, 2013.

[30] J. Labus. Modelling of small capacity absorption chillers driven by solar thermal energy or waste heat. PhD thesis, Universitat Rovira i Virgili, 2011.

[31] J. Sun and S. Zhang. A review of working fluids of absorption cycles. Renewable and Sustainable Energy Reviews, 16:1899–1906, 2012.

[32] RA. Macriss, JM. Gutraj, and TS Zawacki. Absorption fluids data survey: final report on worldwide data. ORNL/Sub/84-47989/3. Institute of Gas Technology. Technical report, Oak Ridge National Laboratory, 1988.

[33] Srikhirin Pongsid, Aphornratana Satha, and Chungpaibulpatana Supachart. A review of absorption refrigeration technologies. Renewable and Sustainable Energy Reviews, 5(4):343–372, 2001.

[34] A. Yokozeki. Theoretical performances of various refrigerant-absorbent pairs in a vapor-absorption refrigeration cycle by the use of equations of state. Applied Energy, 80:383–399, 2005.

[35] L. Hui, NTsoukpoe K. Edem, LP. Nolwenn, and L. Lingai. Evaluation of a seasonal storage system of solar energy for house heating using different absorption couples. Energy Conversion Management, 52:2427–2436, 2011.

[36] KF. Fong, TT. Chow, CK. Lee, Z. Lin, and LS. Chan. Comparative study of different solar cooling systems for buildings in subtropical city. Solar Energy, 84:227–244, 2010.

[37] M. Zamora, M. Bourouis, A. Coronas, and M. Vallès. Pre-industrial development and experimental characterization of a new air-cooled and water-cooled NH3−LiNO3 absorption chiller. International Journal of Refrigeration, 45:189–197, 2014.

[38] B. Prasartkaew. Performance test of a small size LiBr-Water absorption chiller. Energy Procedia, 56:487–497, 2014.

[39] F. Boudéhenn, H. Demasles, J. Wyttenbach, X. Jobard, D. Ch`eze, and P. Papillon. Development of a 5 kw NH3 − water absorption chiller for solar cooling applications. Energy Procedia, 30:35–43, 2012.

[40] Reddy, S. T., Kramer, H. J. M., Lewis, A. E., & Nathoo, J. Investigating factors that affect separation in a eutectic freeze crystallisation process. In International Mine Water Conference, Document Transformation Technologies (2009, October) (pp. 649-655).

[41] Hasan, Mehdi, et al. "Ice growth on the cooling surface in a jacketed and stirred eutectic freeze crystallizer of aqueous Na2SO4 solutions." Separation and Purification Technology 175 (2017): 512-526.

[42] Nathoo, J., R. Jivanji, and A. E. Lewis. "Freezing your brines off: eutectic freeze crystallization for brine treatment." International mine water conference. 2009.